Growth of Single Crystal Graphene Arrays by Locally Controlling Nucleation on Polycrystalline Cu Using Chemical Vapor Deposition

*Wei Wu, Luis A. Jauregui, Zhihua Su, Zhihong Liu, Jiming Bao, Yong P. Chen, and Qingkai Yu**

Graphene, a single atomic layer of hexagonally packed carbon atoms, has drawn significant attention with its outstanding electrical,[1] mechanical,[2,3] and chemical properties.[4,5] Various promising applications based on graphene have been demonstrated, such as in electronics,[6,7] optoelectronics,[8,9] and chemical and biological sensing.[10–12] To further envision graphene technology, it is critical to synthesize high-quality graphene on a large scale. Since the first mechanical isolation of graphene from graphite crystal in 2004,[13] intense efforts have been made to develop methods for graphene synthesis, including reduction of graphene oxide,[14] thermal decomposition of SiC,[15,16] and transition metal assisted chemical vapor deposition (CVD) process.[17–22] In particular, graphene synthesized by CVD on Cu[8,10,17] substrates has shown great promise owing to its large size, high quality, and transferability to arbitrary substrates.

So far, CVD graphene films are polycrystalline, consisting of numerous grain boundaries (Figure S1, Supporting Information).[23,24] A typical CVD process of graphene synthesis on Cu starts with the nucleation of individual graphene grains randomly distributed across the Cu surface. These grains continue to grow with time and eventually merge together to form a continuous polycrystalline film. Recent results have shown that the individual graphene grains before the formation of the continuous film can be a four-lobed polycrystalline single-layer,[24] a hexagonal single crystal single-layer,[25] or a hexagonal single crystal few-layer,[26] depending on CVD parameters. Grain boundaries in graphene have been known to degrade the electrical and mechanical properties of the film.[23,25,27,28] The polycrystalline nature of CVD graphene grown on Cu can be a problem for graphene-based devices because it is unlikely to avoid grain boundaries in the fabricated graphene devices, especially in the case of device arrays and circuits. It is therefore necessary to synthesize either large-scale, high-quality single crystal graphene films, or individual single crystal graphene grains in a controllable arrangement. Recently, Li et al. reported low pressure CVD synthesis of graphene single crystal domains with size up to 0.5 mm on Cu foil.[29] However, the lack of control in domain distribution may still limit further applications. Previously we demonstrated a method to grow single crystal graphene on Cu by CVD from small graphene flakes and to synthesize arrays of graphene grains using pre-patterned multilayer graphene seeds.[25] In that case, however, an extra CVD process was first required to obtain a continuous multilayer graphene film on Cu used for the following lithographic patterning of the growth seeds (multilayer graphene). Here, we propose a more effective approach to control nucleation of CVD graphene by locally providing a high concentration of carbon. In this research, solid carbon source, poly(methyl methacrylate) (PMMA), is used for enhancing local nucleation, and spatially ordered arrays of single crystal graphene grains can be synthesized at predetermined sites (electron beam lithographically patterned arrays of PMMA dots) on the Cu surface. These grains can be transferred to any substrate for further characterization and device fabrication. Our demonstration of controlling locations of graphene nucleation and the synthesis of single crystal graphene arrays could offer a promising route to fabricate graphene-based devices free of grain boundaries and with more reliable performances.

Graphene is synthesized by CVD at ambient pressure on Cu foils covered with PMMA dot arrays (**Figure 1**). The method and transfer procedures are similar to those reported previously.[10] Briefly, annealed Cu foils (25 μm thick) were spin-coated with PMMA film followed by electron beam lithography for patterning dot arrays and used as substrates. Graphene growth was carried out at 1050 °C under 300 sccm Ar (containing 50 ppm CH_4) and 20 sccm H_2 for 20 min in a CVD system. After growth, the graphene material was transferred onto different substrates by a PMMA-assisted wet-transfer method (an aqueous solution of iron nitrate as Cu etchant) for further characterization.

W. Wu
Center for Advanced Materials
University of Houston
Houston, TX 77204, USA
W. Wu, Z. H. Su, Prof. J. M. Bao
Department of Electrical and Computer Engineering
University of Houston
Houston, TX 77204, USA
L. A. Jauregui, Prof. Y. P. Chen
Birck Nanotechnology Center, School of Electrical and Computer Engineering
Department of Physics
Purdue University
West Lafayette, IN 47907, USA
Dr. Z. H. Liu, Prof. Q. K. Yu
Ingram School of Engineering, and Materials Science Engineering and Commercialization Program
Texas State University
San Marcos, TX 78666, USA
E-mail: qingkai.yu@txstate.edu

DOI: 10.1002/adma.201102456

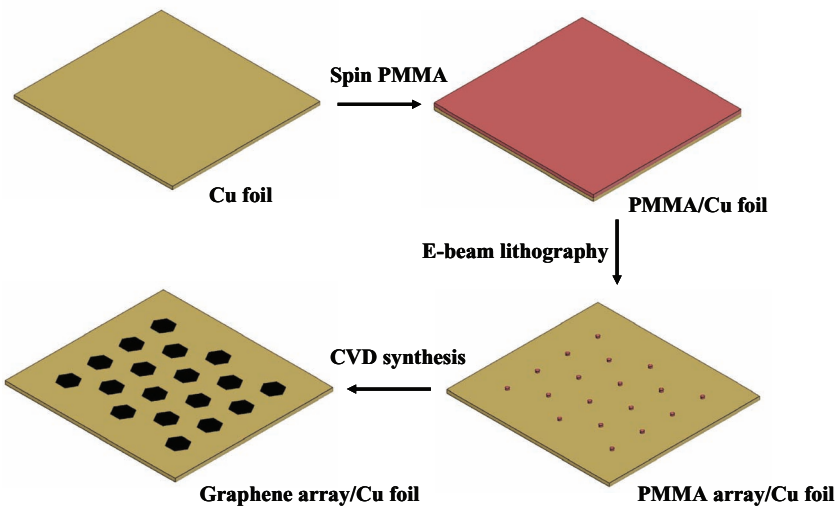

Figure 1. Schematic of growth of graphene arrays on Cu by CVD process at the location with prepatterned PMMA dots.

Figure 2 shows scanning electron microscopy (SEM) images of dots (PMMA) on Cu surface and graphene grains on Cu after CVD process. PMMA dots are circles of ≈0.8 μm in diameter and with a period of 20 μm (Figure 2a). After fabricating the PMMA dot arrays, arrays of graphene grains (areas of dark contrast in Figure 2b,c) are grown on Cu (relatively bright in the images). These grains are observed to have a hexagonal structure with an average size of ≈18 μm, defined as the length of the longest diagonals connecting two opposite vertices. The uniform surface contrast in the images indicates the thickness uniformity of the grains. Our recent work has shown that the hexagonally shaped individual CVD graphene grains before merging together are single crystalline, with edges parallel to the zig-zag orientation.[25] Figure 2d shows an enlarged image of a typical individual graphene grain. The hexagon has well-defined sides, and the underlying microstructures (steps and terraces) of the Cu foil can be observed, but no such features are present in any exposed regions of the foil where graphene has not grown. The exposed regions become oxidized when exposed to air and have been found to be amorphous.[30] This indicates that the graphene grain is protecting the underlying Cu substrate from oxidation.

Raman spectroscopy is a non-destructive and powerful technique to identify the number of layers and presence of defects in graphene.[31,32] In our experiment, Raman spectroscopy and mapping is performed by using a 532 nm excitation laser on CVD grown graphene grains transferred onto SiO_2/Si wafers. Each spectrum is an average of three acquisitions (5 s of accumulation time per acquisition). The intensities (I_x, where x = D, G, or 2D) of the characteristic graphene Raman peaks, D (≈1350 cm^{-1}), G (≈1580 cm^{-1}), and 2D (≈2690 cm^{-1}) are extracted and their spatial dependences (Raman mappings with 0.4 μm spatial and 2.5 cm^{-1} spectral resolutions) are plotted in **Figure 3**a–c for a hexagonally shaped single-layer graphene grain grown at a prepatterned PMMA dot (optical image in Figure 3d). Figure S2a–d (Supporting Information) depicts higher spatial (0.2 μm) and spectral (1 cm^{-1}) resolution Raman mappings of the I_D, I_G, X_G, and $I_{D'}$ respectively, where X_G is the position of the Raman G peak and I_D is the intensity of the characteristic Raman peak D′ peak (≈1620 cm^{-1}). The typical intensity ratio (I_{2D}/I_G) within a grain is larger than 2, indicating that the samples are single-layer graphene.[32] Moreover, I_D is negligible inside most of the grain area, except at a specific region with a diameter of ≈1 μm ± 0.2 μm, which coincides with the location and size of the prepatterned PMMA dot. The region displays a relatively large I_D (location and spectra "a" in **Figure 4**, indicating defects) compared to the spectra from anywhere else inside the grain (location and spectra "b" in Figure 4). It is expected that during the CVD process, the nucleation of graphene occurs at the location of a PMMA dot due to the locally higher concentration of carbon. The specific region with high defect density identified by Raman spectra should be the graphene nucleus. A typical I_D is also observed on the edges (location and spectra "c" in Figure 4), consistent with previous Raman studies of

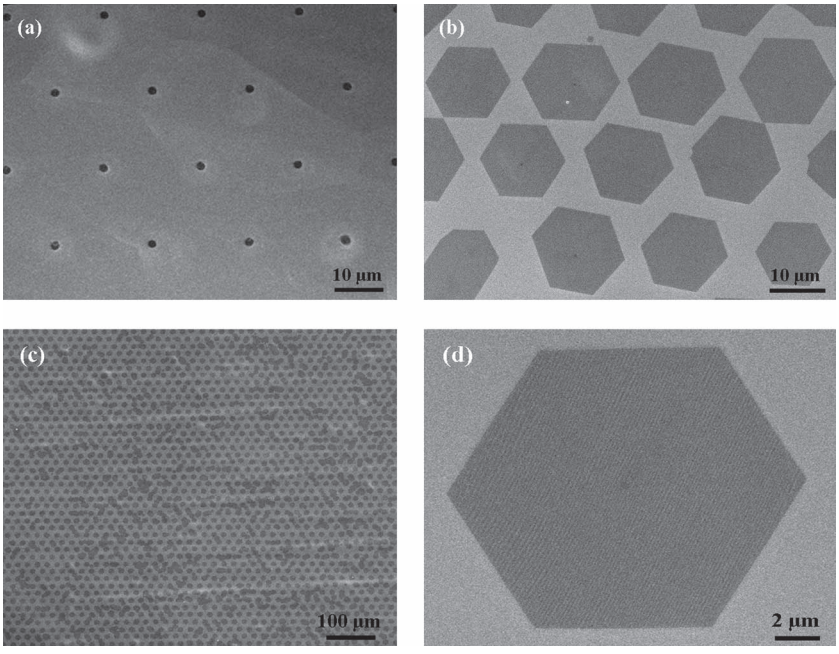

Figure 2. SEM images of a) patterned PMMA dots; b,c) arrays of graphene grains after the CVD process at high and low magnifications, respectively; d) enlarged individual graphene grain. All images were obtained on Cu foils.

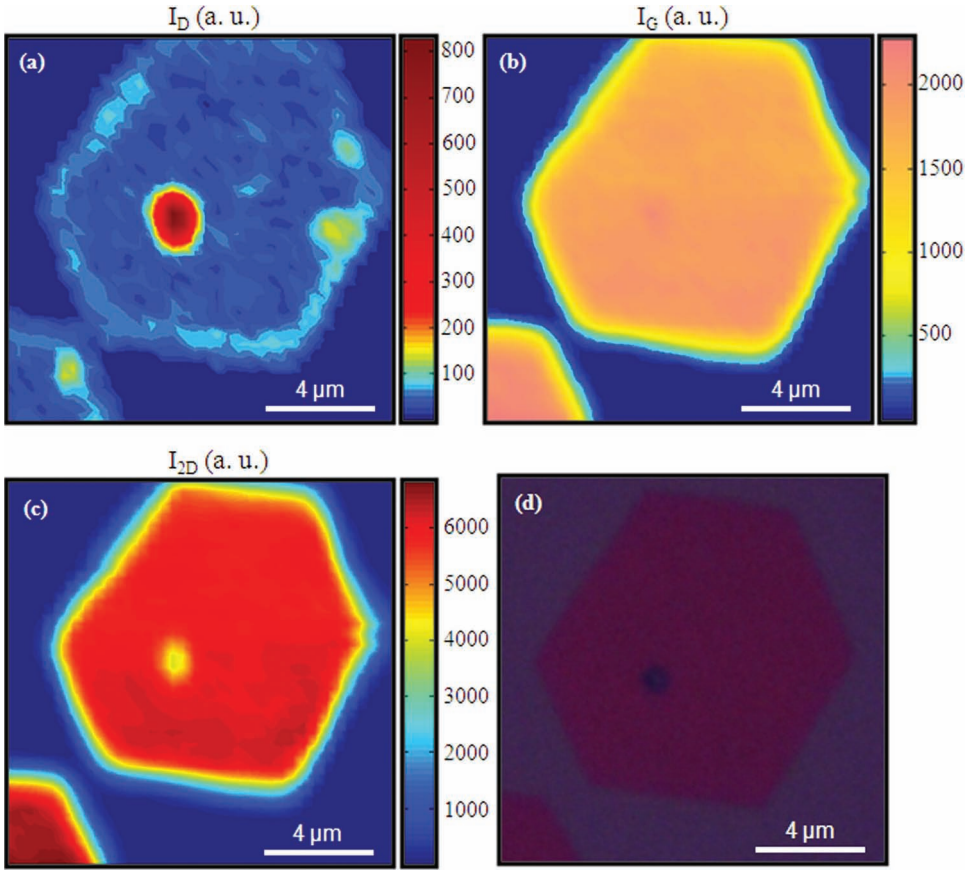

Figure 3. a–c) Intensity mappings of the D, G, and 2D peaks, respectively, for a single crystal graphene grain. The spatial and spectral resolutions of the measurements are 0.4 μm and 2.5 cm^{-1} respectively. d) Optical image of the graphene sample on a SiO_2/Si substrate; the location of nucleus can be seen as a dark spot.

graphene edges.[32,33] Based on the Raman mapping of I_D, grain boundaries are not identified inside the grain, indicating the single crystal nature of these hexagonal graphene grains.[25] On the other hand, Figure S3a–d (Supporting Information) depicts the I_D, I_G, and I_{2D} Raman mappings, and the optical image respectively of a rarely occurring single-layer graphene island (multiple grains) with a non-regular hexagonal shape grown at one single PMMA dot. The Raman mapping of I_D (Figure S3a, Supporting Information) shows the presence of grain boundaries. The occasional observation of such polycrystalline island (multiple nucleation at one site) may be due to the presence of local surface imperfections (pinning sites, folds, or impurities) of the Cu substrate and/or the properties of the specific PMMA dot.

The Raman spectrum inside graphene nucleus (Figure 4a) shows an intensity ratio (I_{2D}/I_G) larger than 1, indicating the presence of ordered carbon (graphene). The spectrum also shows a large intensity ratio ($I_D/I_G \approx 0.4$). Inside the graphene nucleus, the full width at half-maximum (FWHM) of the Raman G band (W_G) is ≈48 cm^{-1} and its peak position (X_G) is 1592.5 cm^{-1} (Figure S2c, Supporting Information). However, anywhere else inside the grain W_G is ≈20 cm^{-1} (Figure 4b) and X_G is 1583 cm^{-1} (Figure S2c, Supporting Information). Such a difference in peak position and width of the Raman G peak was found in studies of disordered carbon.[31] The disordered carbon in this case may be formed during the decomposition of PMMA at elevated temperature. We also observe the presence of the Raman D′ peak at ≈1620 cm^{-1} inside the graphene nucleus after fitting the Raman G peak with two Lorentzian functions. The Raman D′ peak indicates an (elastic) intravalley scattering process and it has been observed in samples with a considerable number of defects.[31,32]

After transferring graphene grains from the Cu foil to SiO_2 by the PMMA-assisted method, we protected the chosen grains by negative electron beam resist (MA-N 2403). Then, everywhere else was etched by O_2 plasma to avoid shortening of the electrical contacts by other graphene grains. The electrical contacts (Cr/Au, 5 nm/35 nm, electron beam evaporated) to graphene grains are patterned by electron beam lithography, a typical device is depicted in Figure S4a (Supporting Information). The intragrain mobility (μ_G) extracted from low-temperature Hall measurements in all of the devices we studied ranged from $<10^3$ cm^2 V^{-1} s^{-1} to ≈10^4 cm^2 V^{-1} s^{-1} (Figure S4b, Supporting Information). Our previous work clearly indicated the detrimental effect of grain boundaries on electronic transport and that avoiding grain boundaries is beneficial for improving the mobility.[25] However, the wide variation of μ_G in different samples and the occasional low μ_G observed

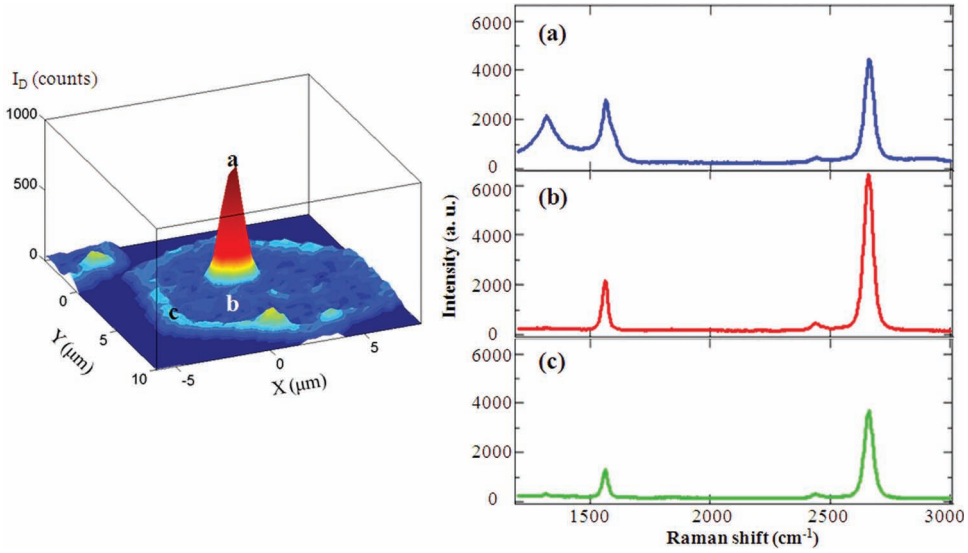

Figure 4. False-color 3D plots of the spatially dependent Raman D peak intensity (I_D). Individual Raman spectra taken from three representative locations: a) on a defect site, artificial nucleation center, b) inside the single crystal graphene grain, and c) on the edge of graphene.

suggest that other sources of disorder could also strongly affect the mobilities. Improving related fabrication processes to reduce such defects will be required to achieve consistent high mobilities in graphene-based devices.

Substrate surface seeding has been a common surface pretreatment method used to modify and control the surface nucleation density and the rate of diamond films.[34] Seeds, i.e., submicrometer diamond powder or particles, littered on the substrate surface are the predominant nucleation sites and/or they, themselves, are nuclei for immediate growth. In our case, we applied arrays of PMMA dots to generate graphene nuclei for the growth of single crystal graphene arrays. At high temperature (1050 °C), the precursor CH_4 is adsorbed on Cu surface and decomposed to form active carbon species (C adatoms) catalyzed by Cu. Because of the extremely low solubility of carbon in Cu, the formed C adatoms will diffuse largely on the surface and gradually build up the C adatom concentration. Once a supersaturation (locally at the sites of PMMA dots) is achieved, graphene nucleation preferentially occurs on the PMMA sites due to the locally higher concentration of C adatoms, and individual graphene grains grow.

In a general growth process for CVD graphene on Cu substrate, i.e., annealed Cu foil and no artificial seeds or prepatterned solid carbon source, spontaneous nucleation of graphene grains is expected and occurs only when a large C adatom supersaturation has been reached on the Cu surface. The nucleation is believed to be uniform and grains are randomly distributed all over the substrate (Figure S1, Supporting Information). The growth of graphene grains then consumes C adatoms, decreasing their concentration, until equilibrium is established among the graphene, the Cu surface, and the C vapor phase. Loginova et al. found that the C adatom concentration needed for the spontaneous nucleation of graphene grains on Ru and Ir surfaces is about twice the equilibrium concentration and graphene only grows above equilibrium.[35,36] By taking advantage of the required large C adatom supersaturation for the spontaneous nucleation, we purposely introduced PMMA dots as designated nucleation sites. Upon CH_4 decomposition on Cu, interrupted nucleation of graphene grains preferentially at the PMMA sites occurs because of the locally higher C adatom concentration. It has been demonstrated that polymer films or small molecules (PMMA or fluorene) are good solid carbon sources for producing high-quality graphene.[37]

The amount of PMMA used to generate nucleus critically influence graphene nucleation process. High-quality arrays of single crystal single-layer graphene grains are obtained using PMMA dots of ≈0.8 μm in diameter and ≈0.4 μm in thickness as discussed above. Occasionally, multiple graphene grains, i.e., polycrystalline islands, nucleated and grown from one single such nucleus are also observed (Figure S3, Supporting Information). The multinucleation of graphene at individual sites is largely related to properties of the PMMA dots. **Figure 5**a shows a SEM image of graphene arrays grown from ≈2 μm diameter PMMA dots with the same thickness of ≈0.4 μm. The individual islands have irregular shapes instead of the hexagonal structures and can be mostly determined to be polycrystalline, consisting of multiple grains (Figure 5a inset). The dark areas on each island indicate few-layer graphene domains, which are formed from the increased amount of solid carbon precursor (PMMA). When the thickness of the 2 μm diameter PMMA dots increases to ≈2 μm, a continuous graphene film with arrays of few-layer domains are formed after the same CVD process (Figure 5b). Residues of the PMMA after growth can also be clearly observed, shown as white dots in the image. It is believed that the large amount of PMMA has contributed to the growth of this relatively large area film with many thick domains.[37] With careful control of the amount of PMMA used, it demonstrates a potential to grow graphene films with patterned bi- or few-layer domains.

In addition, we also use pieces of highly oriented pyrolytic graphite (HOPG) as seeds transferred on Cu foils to grow graphene grains under the same growth conditions as

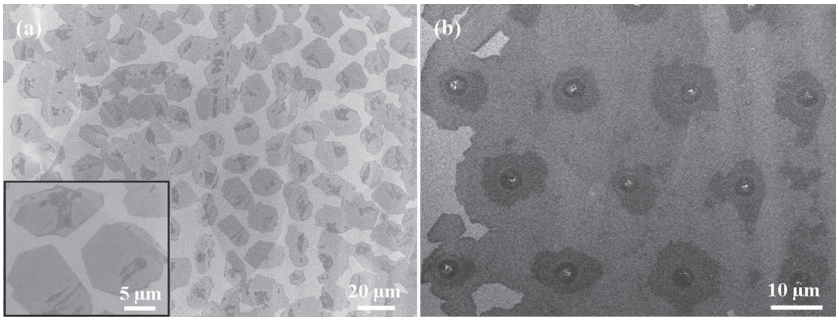

Figure 5. SEM images of a) arrays of graphene islands consisting of multiple grains grown from PMMA dots with ≈2 μm in diameter and ≈0.4 μm in thickness. The inset shows individual islands at high magnification. b) Continuous graphene films with arrays of thick domains grown from ≈2 μm diameter PMMA dots but with a thickness of ≈2 μm. All images were obtained on Cu foils.

were used in the case of PMMA. An array of graphite micropillars was first fabricated on HOPG surface according to refs.[38] and [39] (Figure S5, Supporting Information). Since graphite can be easily cleaved along its basal planes, individual thin plates of multiple or single graphite layers are then transferred onto surfaces of Cu foils, simply by pressing against the patterned HOPG. After the CVD synthesis, a preferential nucleation of graphene on HOPG sites is also observed (Figure S6,S7, Supporting Information). However, due to the roughness and flexibility of the surfaces of such thin Cu foils (25 μm in thickness), transferred graphite plates differ significantly in size and thickness, which will largely affect graphene growth. In addition, it is very difficult to fabricate well-defined arrays of HOPG seeds on Cu surface through the pressing transfer technique.

In summary, we have demonstrated control of the nucleation of CVD graphene on Cu by prepatterned solid carbon source and the growth of arrays of single crystal graphene grains. SEM and Raman spectroscopy characterizations confirm the hexagonal structure and single crystal nature of the graphene grains. Electrical transport measurements show the grains have good mobilities. These synthesis method could lead to a new technology for fabricating graphene-based devices that are free of grain boundaries and that have better performances.

Experimental Section

Cu Surface Pretreatment: Cu foils (25 μm thick, 99.8%, Alfa) were first thoroughly cleaned with acetone, methanol, and deionized (DI) water and annealed at 1000 °C for 30 min in the protection of Ar and H_2. A thin layer of PMMA (MicroChem 950 PMMA C, 3% in chlorobenzene) was spin-coated on the Cu surface at 3000 rpm for 1 min, which was then cured at 150 °C for 2 min. The thickness of the PMMA film was ≈400 nm. Subsequently, the PMMA-coated sample was subject to electron beam lithography where the PMMA was used as a negative resist. After being irradiated by a higher dose, exposed PMMA molecules crosslinked with each other to form a network of larger molecules that remained during the developing process (acetone, methanol, and DI water), while the other unexposed areas were washed away. A well-defined PMMA dot arrays on the Cu surface was then obtained.

Graphene Synthesis and Transfer: Cu foils covered with PMMA pattern were loaded into a CVD furnace as the growth substrates. Afterwards, the system was thoroughly evacuated by mechanical pump and turbomolecular pump to reach a base pressure of ≈10^{-5} Torr and then quickly back-filled with Ar and H_2 to ambient pressure. The furnace was heated up to 1050 °C in 3 h under 300 sccm Ar and 20 sccm H_2. Subsequently, graphene growth was carried out at 1050 °C under a gas mixture of 300 sccm (containing 50 ppm CH_4) and 20 sccm H_2 for 20 min. Finally, the samples were rapidly cooled down to room temperature in the protection of Ar and H_2.

After growth, graphene material was transferred by a PMMA-assisted wet-transfer method on 300 nm SiO_2/Si wafer for Raman spectroscopy and electrical transport measurements. A thin layer of PMMA (MicroChem 950 PMMA C, 3% in chlorobenzene) was spin-coated on an as-synthesized sample at 3000 rpm for 1 min, which was then cured at 150 °C for 2 min. Since both Cu surfaces were exposed to CH_4, graphene was grown on both sides of the Cu foil. Graphene on the Cu surface without PMMA cover was removed by O_2 plasma etching. Subsequently, the sample was placed in an aqueous solution of iron nitrate (0.1 g mL^{-1}) to etch off the Cu foil. Typically, the etching process runs overnight. After the Cu foil was completely etched away, graphene with PMMA coating was scooped out from the solution by the transfer substrate. The PMMA was then removed with acetone and the sample was rinsed several times with DI water. During the transfer process, the arrangement of as-synthesized graphene grains was maintained by the supporting PMMA layer. After transferred on target substrate (SiO_2/Si in this case), graphene grains were closely attached to the substrate so that they could keep their original arrangement, even when PMMA was eventually removed.

Supporting Information

Supporting Information is available from the Wiley Online Library or from the author.

Acknowledgements

The authors acknowledge support from the NSF and UHCAM. J.M.B. acknowledges support from the Robert A. Welch Foundation (E-1728) and the NSF under Grant No. DMR-0907336.

Received: June 28, 2011
Revised: August 9, 2011
Published online: September 23, 2011

[1] A. K. Geim, K. S. Novoselov, *Nat. Mater.* **2007**, *6*, 183.
[2] J. S. Bunch, A. M. van der Zande, S. S. Verbridge, I. W. Frank, D. M. Tanenbaum, J. M. Parpia, H. G. Craighead, P. L. McEuen, *Science* **2007**, *315*, 490.
[3] D. Garcia-Sanchez, A. M. van der Zande, A. S. Paulo, B. Lassagne, P. L. McEuen, A. Bachtold, *Nano Lett.* **2008**, *8*, 1399.
[4] F. Schedin, A. K. Geim, S. V. Morozov, E. W. Hill, P. Blake, M. I. Katsnelson, K. S. Novoselov, *Nat. Mater.* **2007**, *6*, 652.
[5] T. O. Wehling, K. S. Novoselov, S. V. Morozov, E. E. Vdovin, M. I. Katsnelson, A. K. Geim, A. I. Lichtenstein, *Nano Lett.* **2008**, *8*, 173.
[6] M. C. Lemme, T. J. Echtermeyer, M. Baus, H. Kurz, *IEEE Electron Device Lett.* **2007**, *28*, 282.
[7] Y. M. Lin, C. Dimitrakopoulos, K. A. Jenkins, D. B. Farmer, H. Y. Chiu, A. Grill, P. Avouris, *Science* **2010**, *327*, 662.

[8] S. Bae, H. Kim, Y. Lee, X. F. Xu, J. S. Park, Y. Zheng, J. Balakrishnan, T. Lei, H. R. Kim, Y. I. Song, Y. J. Kim, K. S. Kim, B. Ozyilmaz, J. H. Ahn, B. H. Hong, S. Iijima, *Nat. Nanotechnol.* **2010**, *5*, 574.
[9] X. Wang, L. J. Zhi, N. Tsao, Z. Tomovic, J. L. Li, K. Mullen, *Angew. Chem. Int. Ed.* **2008**, *47*, 2990.
[10] W. Wu, Z. H. Liu, L. A. Jauregui, Q. K. Yu, R. Pillai, H. L. Cao, J. M. Bao, Y. P. Chen, S. S. Pei, *Sens. Actuators B* **2010**, *150*, 296.
[11] Y. Ohno, K. Maehashi, Y. Yamashiro, K. Matsumoto, *Nano Lett.* **2009**, *9*, 3318.
[12] N. Mohanty, V. Berry, *Nano Lett.* **2008**, *8*, 4469.
[13] K. S. Novoselov, A. K. Geim, S. V. Morozov, D. Jiang, Y. Zhang, S. V. Dubonos, I. V. Grigorieva, A. A. Firsov, *Science* **2004**, *306*, 666.
[14] S. Park, R. S. Ruoff, *Nat. Nanotechnol.* **2009**, *4*, 217.
[15] C. Berger, Z. M. Song, T. B. Li, X. B. Li, A. Y. Ogbazghi, R. Feng, Z. T. Dai, A. N. Marchenkov, E. H. Conrad, P. N. First, W. A. de Heer, *J. Phys. Chem. B* **2004**, *108*, 19912.
[16] C. Berger, Z. M. Song, X. B. Li, X. S. Wu, N. Brown, C. Naud, D. Mayou, T. B. Li, J. Hass, A. N. Marchenkov, E. H. Conrad, P. N. First, W. A. de Heer, *Science* **2006**, *312*, 1191.
[17] X. S. Li, W. W. Cai, J. H. An, S. Kim, J. Nah, D. X. Yang, R. Piner, A. Velamakanni, I. Jung, E. Tutuc, S. K. Banerjee, L. Colombo, R. S. Ruoff, *Science* **2009**, *324*, 1312.
[18] Q. K. Yu, J. Lian, S. Siriponglert, H. Li, Y. P. Chen, S. S. Pei, *Appl. Phys. Lett.* **2008**, *93*, 113103.
[19] A. Reina, X. T. Jia, J. Ho, D. Nezich, H. B. Son, V. Bulovic, M. S. Dresselhaus, J. Kong, *Nano Lett.* **2009**, *9*, 30.
[20] P. W. Sutter, J. I. Flege, E. A. Sutter, *Nat. Mater.* **2008**, *7*, 406.
[21] J. Coraux, A. T. N'Diaye, C. Busse, T. Michely, *Nano Lett.* **2008**, *8*, 565.
[22] S. J. Chae, F. Gunes, K. K. Kim, E. S. Kim, G. H. Han, S. M. Kim, H. J. Shin, S. M. Yoon, J. Y. Choi, M. H. Park, C. W. Yang, D. Pribat, Y. H. Lee, *Adv. Mater.* **2009**, *21*, 2328.
[23] X. S. Li, C. W. Magnuson, A. Venugopal, J. H. An, J. W. Suk, B. Y. Han, M. Borysiak, W. W. Cai, A. Velamakanni, Y. W. Zhu, L. F. Fu, E. M. Vogel, E. Voelkl, L. Colombo, R. S. Ruoff, *Nano Lett.* **2010**, *10*, 4328.
[24] J. M. Wofford, S. Nie, K. F. McCarty, N. C. Bartelt, O. D. Dubon, *Nano Lett.* **2010**, *10*, 4890.
[25] Q. K. Yu, L. A. Jauregui, W. Wu, R. Colby, J. F. Tian, Z. H. Su, H. L. Cao, Z. H. Liu, D. Pandey, D. G. Wei, T. F. Chung, P. Peng, N. Guisinger, E. A. Stach, J. M. Bao, S. S. Pei, Y. P. Chen, *Nat. Mater.* **2011**, *10*, 443.
[26] A. W. Robertson, J. H. Warner, *Nano Lett.* **2011**, *11*, 1182.
[27] P. Y. Huang, C. S. Ruiz-Vargas, A. M. van der Zande, W. S. Whitney, M. P. Levendorf, J. W. Kevek, S. Garg, J. S. Alden, C. J. Hustedt, Y. Zhu, J. Park, P. L. McEuen, D. A. Muller, *Nature* **2011**, *469*, 389.
[28] L. Gao, J. R. Guest, N. P. Guisinger, *Nano Lett.* **2010**, *10*, 3512.
[29] X. Li, C. W. Magnuson, A. Venugopal, R. M. Tromp, J. B. Hannon, E. M. Vogel, L. Colombo, R. S. Ruoff, *J. Am. Chem. Soc.* **2011**, *133*, 2816.
[30] J. Cho, L. Gao, J. F. Tian, H. L. Cao, W. Wu, Q. K. Yu, E. N. Yitamben, B. Fisher, J. R. Guest, Y. P. Chen, N. P. Guisinger, *ACS Nano* **2011**, *5*, 3607.
[31] A. C. Ferrari, *Solid State Commun.* **2007**, *143*, 47.
[32] A. C. Ferrari, J. C. Meyer, V. Scardaci, C. Casiraghi, M. Lazzeri, F. Mauri, S. Piscanec, D. Jiang, K. S. Novoselov, S. Roth, A. K. Geim, *Phys. Rev. Lett.* **2006**, *97*, 187401.
[33] L. M. Malard, M. A. Pimenta, G. Dresselhaus, M. S. Dresselhaus, *Phys. Rep.-Rev. Sec. Phys. Lett.* **2009**, *473*, 51.
[34] F. Jansen, M. A. Machonkin, D. E. Kuhman, *J. Vac. Sci. Technol. A-Vac. Surf. Films* **1990**, *8*, 3785.
[35] E. Loginova, N. C. Bartelt, P. J. Feibelman, K. F. McCarty, *New J. Physics* **2008**, *10*, 093026.
[36] E. Loginova, N. C. Bartelt, P. J. Feibelman, K. F. McCarty, *New J. Physics* **2009**, *11*, 063046.
[37] Z. Z. Sun, Z. Yan, J. Yao, E. Beitler, Y. Zhu, J. M. Tour, *Nature* **2010**, *468*, 549.
[38] X. K. Lu, M. F. Yu, H. Huang, R. S. Ruoff, *Nanotechnology* **1999**, *10*, 269.
[39] D. S. Li, W. Windl, N. P. Padture, *Adv. Mater.* **2009**, *21*, 1243.